

A Highly Effective Deflecting Structure

C. Leemann, C. G. Yao

Abstract: A structure is presented that combines high transverse shunt impedance with outside dimensions that are small in relation to the desired mode's resonant frequency. The basic idea was to find a practical way to resonate a small gap, two conductor, $\lambda/4$ transmission line with a field pattern that is locally very close to a TEM dipole mode (apart from important and essential modifications at the gap end). Two applications stand out: use an RF separator (discussed here) or use as a high sensitivity microwave BPM.

The basic structure is shown in Figure 1. It is a $1/4$ wavelength resonator. Two rods are placed along the Z direction. There are gaps between the rods and the cavity wall on one side. The mode being used to deflect the electrons is a dipole mode, field patterns of which are shown in Figures 2-5. The gaps are essential to excite this mode.

The rods play an important role in two aspects. First, they cut down the outside cavity diameter. For example, the outside diameter of a disk loaded waveguide for a 500 MHz deflecting cavity is about 800 mm, but with the proposed cavity, it can be as small as 120 mm. Second, they compress the field into the central region of the cavity, so that the fields in the central region of the cavity are very high which leads to very high transverse shunt impedance R_{\perp} . For example, for a square box deflecting cavity such as the CEBAF chopper, $R_{\perp} \approx 2.8 \text{ M}\Omega/\text{m}$, and for a biperiodic structure of current CEBAF RF separator design $R_{\perp} \approx 15 \text{ M}\Omega/\text{m}$, but for this $1/4$ wavelength resonator the R_{\perp} ranges from 200 to 500 $\text{M}\Omega/\text{m}$ depending on detailed choice of geometry.

We use MAFIA to calculate the properties of this type of cavity. The dimensions of the cavity under study are the following:

$$\begin{aligned} \text{cavity length } l_c &= 150 \text{ mm} \\ \text{beam aperture } d_{in} &= 20 \text{ mm} \\ \text{rod diameter } d &= 20 \text{ mm} \end{aligned}$$

Figure 6 shows the relationship between the frequency and gap width. As the gap gets larger, the frequencies of the modes go higher for all three modes.

Figure 7 and Figure 8 show the transverse shunt impedance R_{\perp} and Q value vs. gap width. As gap width is decreased, the transverse shunt impedance R_{\perp} goes up and Q goes down.

As expected, when the two rods get closer to each other, the transverse shunt impedance rapidly increases (Figure 9).

Since this is a $1/4$ wavelength resonator, it is expected that the frequency of the mode strongly depends on the rod length (or gap width) rather than the outside diameter of the cavity (Figure 10).

In some applications only one single cavity need be used. However, to make this type of cavity useful for the CEBAF RF separators that require a very strong deflection effect, it may be desirable to find a way to couple them together.

The field patterns in Figures 2 and 3 show that the electric field is perpendicular to the plane S and the magnetic field is very weak in the region close to the plane S . If the two $1/4$ wavelength cells are put together facing each other as shown in Figure 10, and the plane S is taken away to form a $1/2$ wavelength cavity (π mode), the field pattern will almost be unaffected, and its performances (frequency, R_{\perp} , etc.) will remain the same as a single $1/4$ wavelength cell. Furthermore, we are able to couple several of these cavities together through slots in the webs to constitute a structure. Figure 12 shows an example of two cavities coupled together. This is a structure with magnetic coupling. It has backward wave property. The frequency of 0 mode is higher than that of π mode. An increase in slot size will enlarge the separation of the modes. Figures 13 to 15 show field patterns of E and B along the structure of 0 and π modes, respectively.

After careful optimization of cavity geometry the effective transverse shunt impedance R_{\perp} over the whole structure, which is 60 cm long and operated at 500 MHz, is around 500 M Ω /m. The Q value of the structure is ≈ 10000 . If this structure is used as an RF separator for the highest energy (5 GeV), the required RF power is:

$$p = \frac{(5 \text{ GeV} \times 10^{-4} \times 1.16)^2}{RL} = 1.1 \text{ kW.}$$

By comparison, the current design RF separator for the highest energy is ≈ 3 m long and requires 10 kW of RF power.

It can be seen from the field pattern that a large part of power dissipation is on the surface of the rods and the web, and special attention should be paid to cooling these parts of the structure.

Figure 16 shows the field uniformity in the central region of the structure. As can be seen the fields in the central region are more uniform with bigger rods. The phase space distortion caused by the deflecting structure is less than 1% if the beam size is about 1 mm in diameter. Finally, the field pattern is sextupole-like; any phase space distortion caused by the structure may presumably be corrected by a sextupole magnet placed with an appropriate phase advance downstream of the separator.

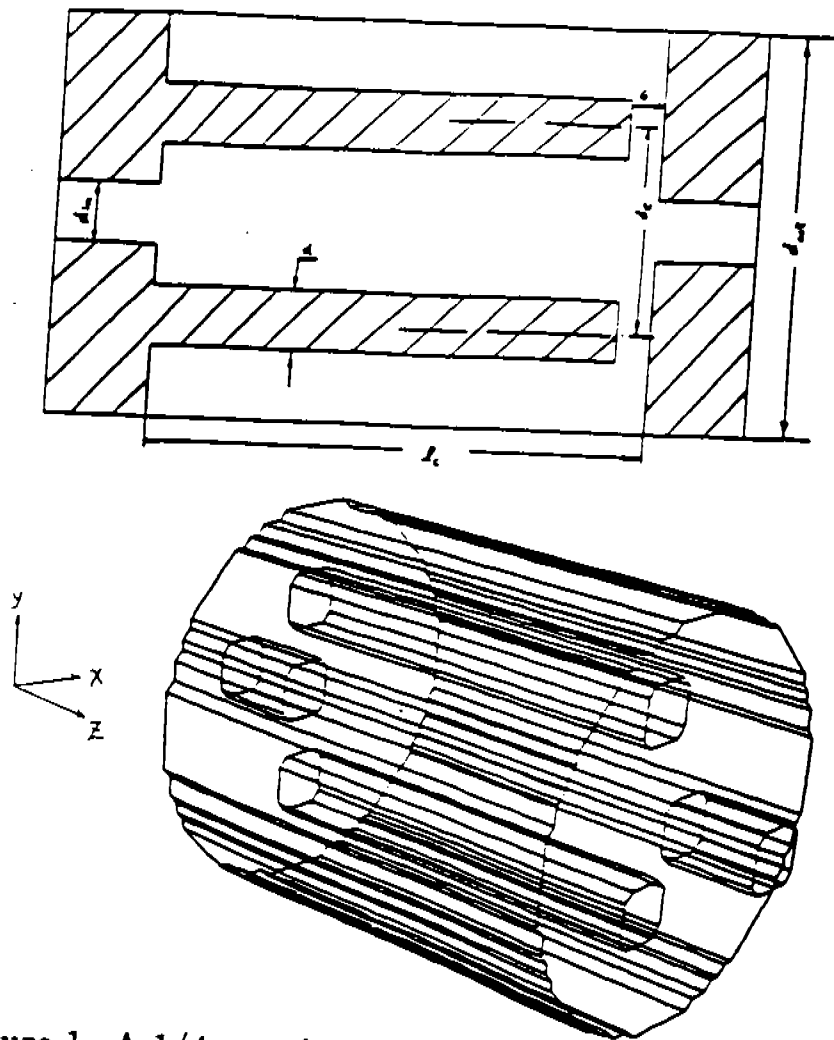


Figure 1. A $\frac{1}{4}$ wavelength resonator of the dipole mode.

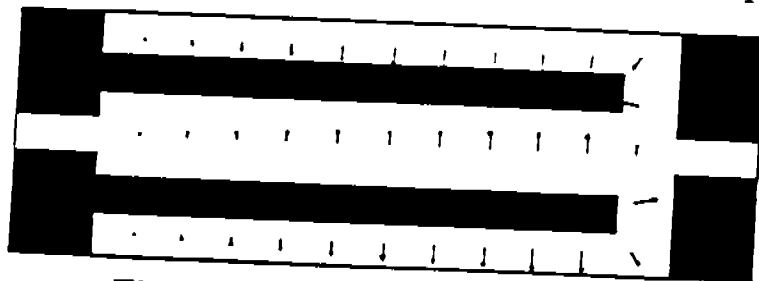


Figure 2. E field in $y-z$ plane. \vec{S}

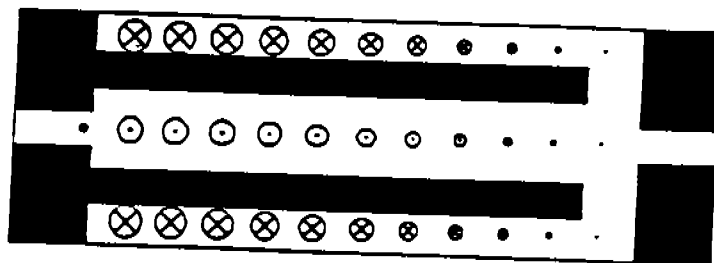


Figure 3. B field in $y-z$ plane. \vec{S}

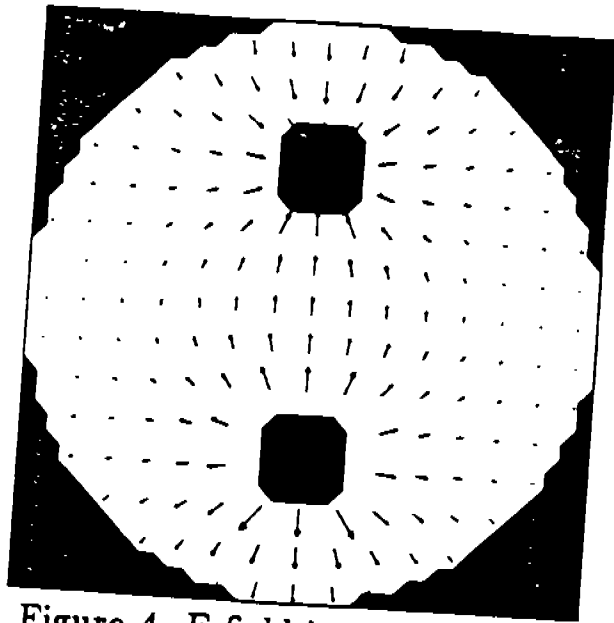


Figure 4. E field in x - y plane.

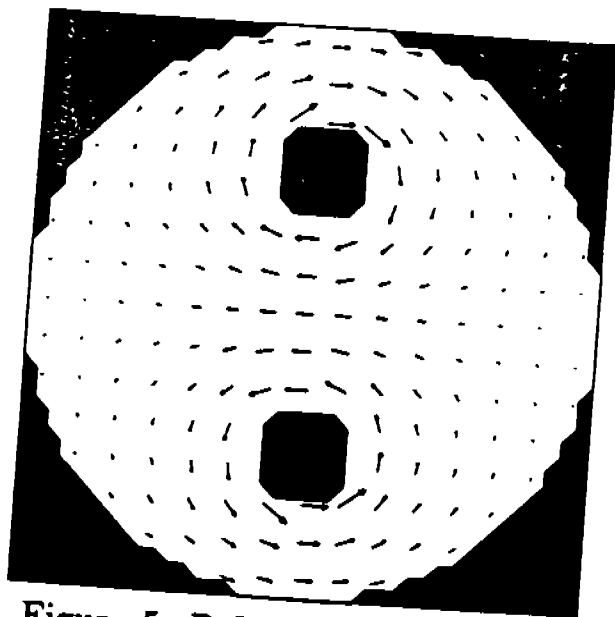


Figure 5. B field in x - y plane.

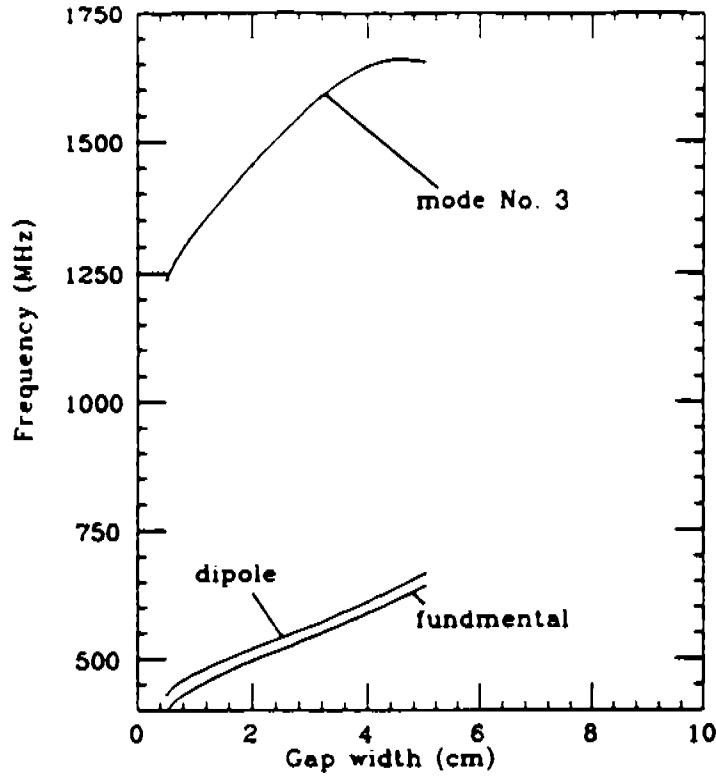


Figure 6. Frequencies of three modes vs. gap width.

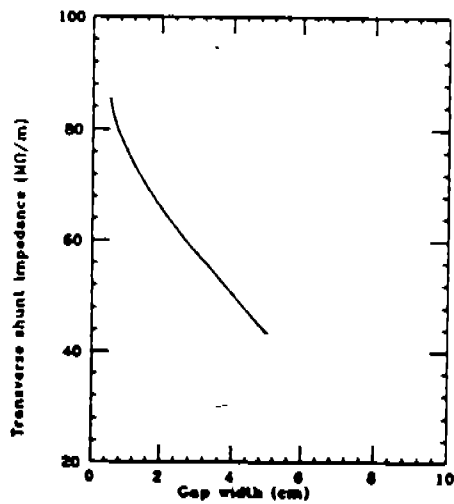


Figure 7. Transverse shunt impedance vs. gap width.

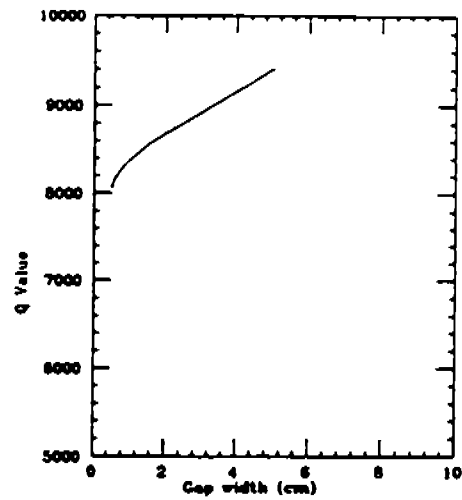


Figure 8. Q value vs. gap width.

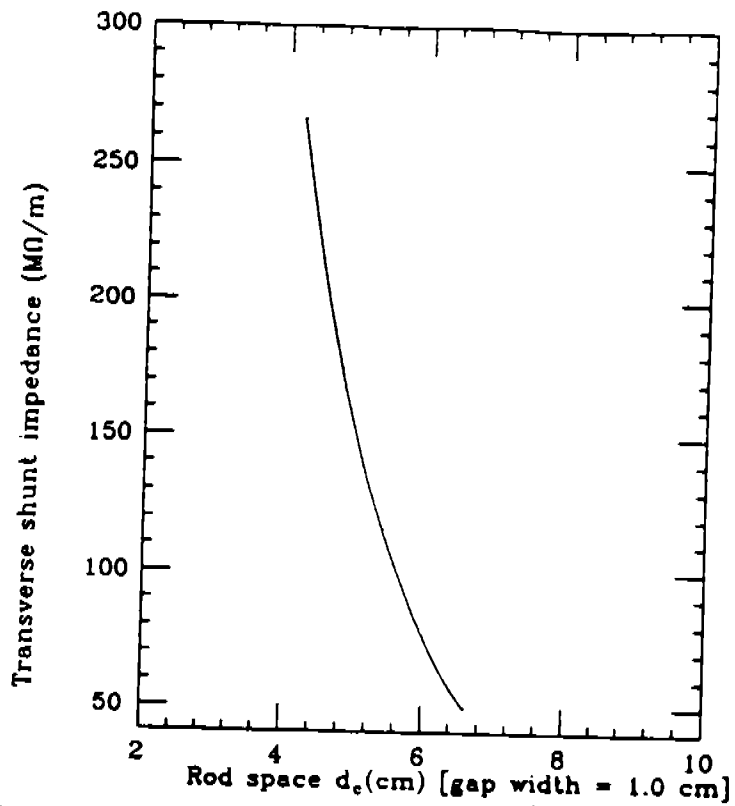


Fig. 9 Transverse shunt impedance vs. Rod space ($D_{rod}=2cm$)

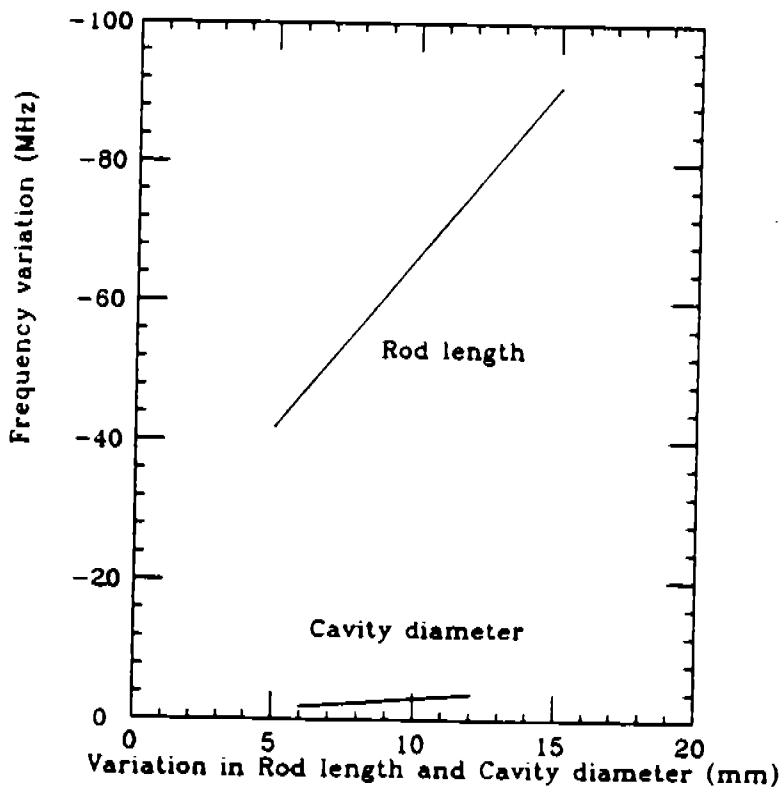


Fig. 10 Frequency variation vs. Rod length and Cavity diameter

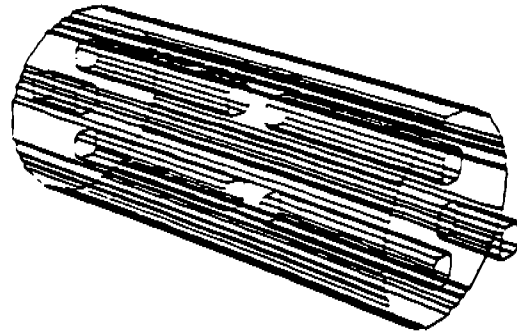
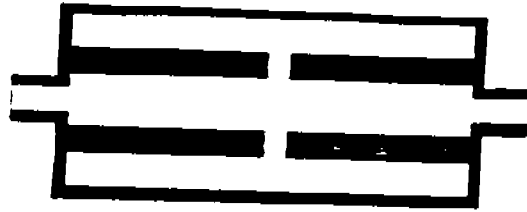


Figure 11. A π mode cavity consisting of two $1/4$ wavelength cells.

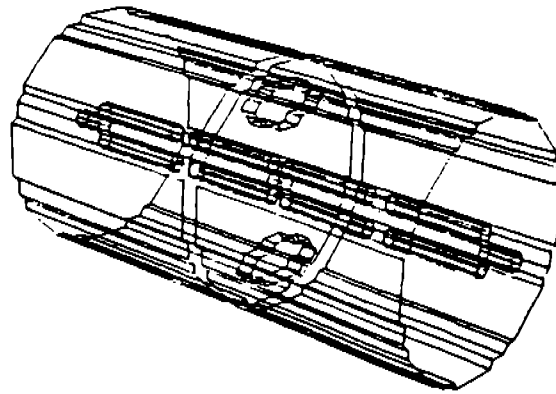


Figure 12. A highly effective deflecting structure.

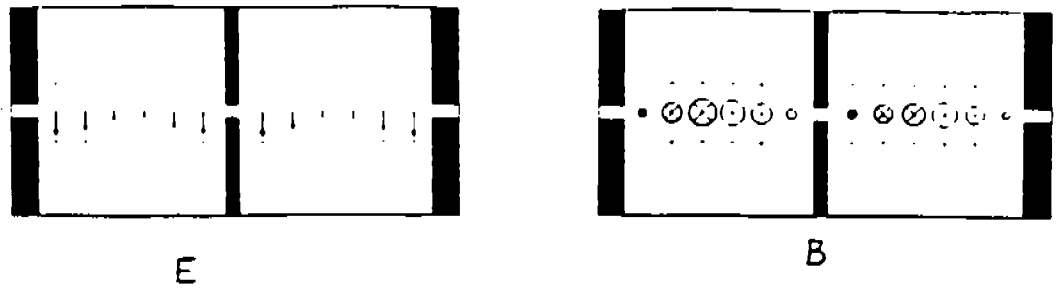


Figure 13. E and B field on x - z plane for 0 mode.

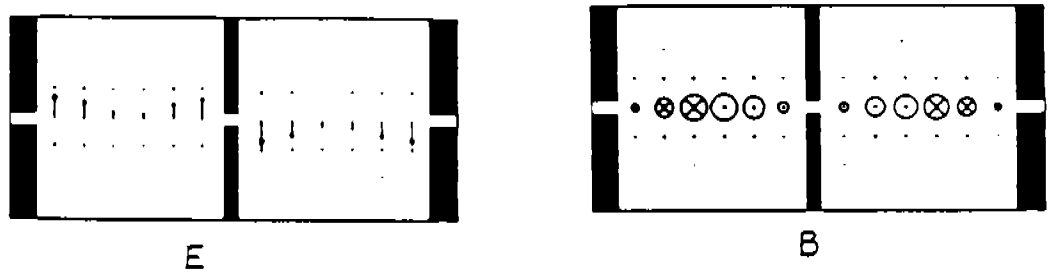


Figure 14. E and B field on x - z plane for π mode.

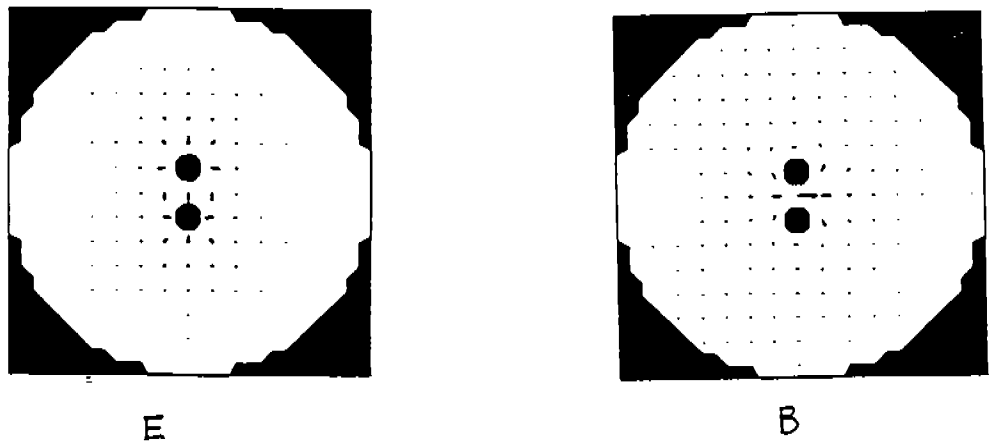


Figure 15. E and B field on x - y plane for π mode.

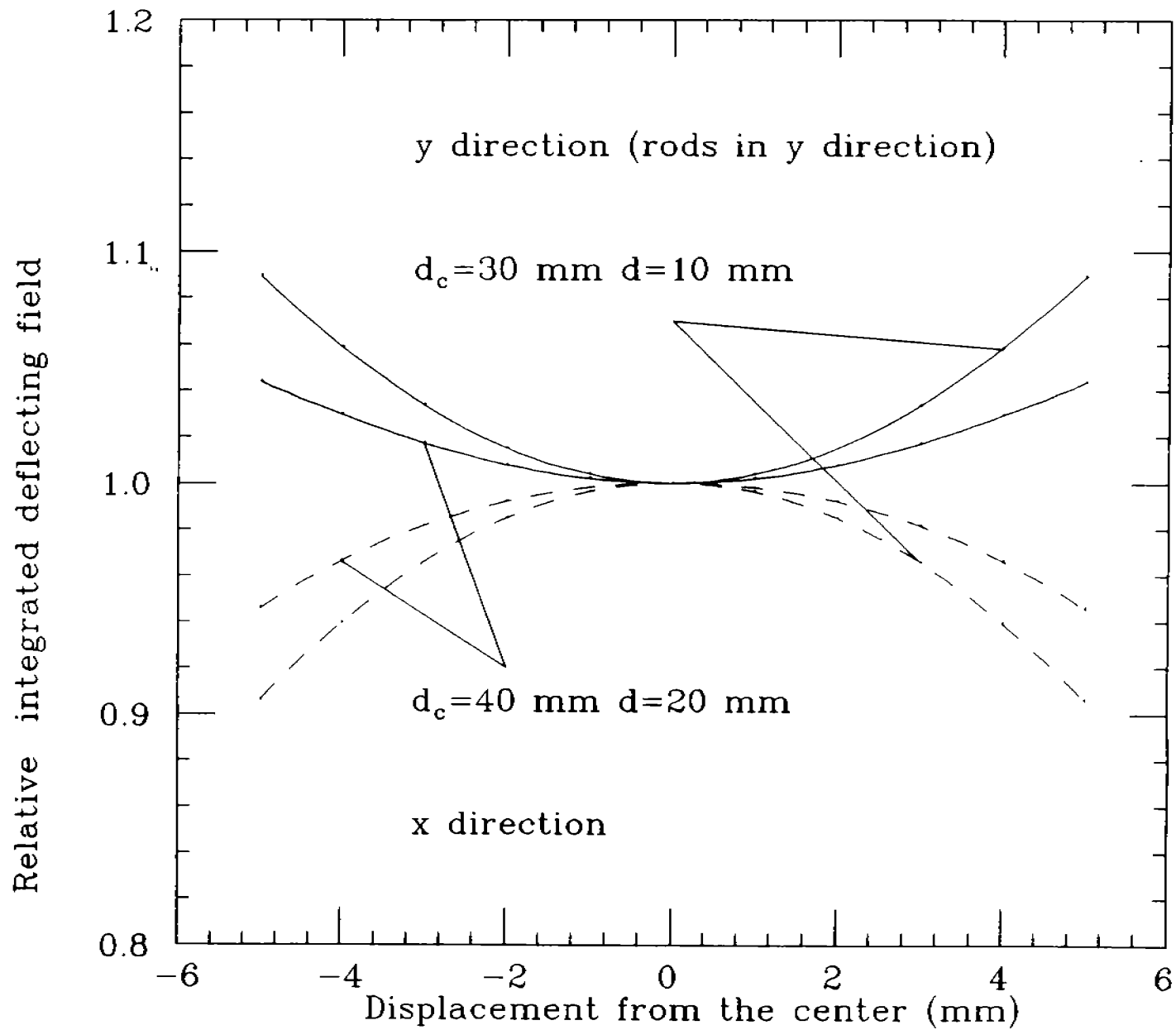


Figure 16. field uniformity in central region